High accuracy magnetic field sensors with wide operation temperature range

I S Vasil'evskii[1], A N Vinichenko[1], D I Rubakin[1], I A Bolshakova[2] and N I Kargin[1]

[1]National Research Nuclear University MEPhI, (Moscow Engineering Physics Institute), Kashirskoe shosse 31, 115409 Moscow, Russian Federation
[2]Lviv Polytechnic National University, Bandera street 12, 79013 Lviv, Ukraine

Corresponding author e-mail address: ivasilevskii@mail.ru

Abstract. n+InAs(Si) epitaxial thin films heavily doped by silicon and Hall effect magnetic field sensors based on this structures have been fabricated and studied. We have demonstrated the successful formation of highly doped InAs thin films (~100 nm) with the different intermediate layer arrangement and appropriate electron mobility values. Hall sensors performance parameters have been measured in wide temperature range. Obtained sensitivity varied from 1 to 40 Ω/T, while the best linearity and lower temperature coefficient have been found in the higher doped samples with lower electron mobility. We attribute this to the electron system degeneracy and decreased phonon contribution to electron mobility and resistance.

1. Introduction

Magnetic field sensors are widely used in MegaScience research projects as the magnetic field is used as a key tool for the control of charged particle beams. In various magnetic field control systems, the high precision magnetic field sensors must have good linearity over a wide range of magnetic field (1 ÷ 8 T), the low drift of sensitivity and resistance over a wide temperature range - from cryogenic to high (4,2 ÷ 600 K). Furthermore, the sensors should be compact in size. For a number of experimental systems, an additional requirement is a long-term stable operation of such sensors in conditions of charged particles, neutrons and gamma rays radiation [1,2]. Traditional silicon sensors cannot withstand such operating conditions.

A3B5 compound semiconductors offer an advanced performance due to high electron mobility, high electron density and thin film technology. Among them InAs and InSb thin film heterostructures are most attractive due to high doping level, providing the electron degeneracy and thus, low temperature drift [3,4]. However, the mechanical deformations due to the mismatch of the lattice constants of GaAs substrate and InAs or InSb make difficult to obtain high-quality InAs layers during epitaxial growth. Direct overgrowth of InAs causes propagation of the dislocations from nucleation layer to the overlying heterostructure active layers, enhancing the scattering of electrons, thus increasing the device resistivity. In the direct epitaxial growth of the relaxed InAs films, the dislocations' density decreases quickly with an increase of film thickness, and the quality improvement is observed with a layer thickness of $> 1.5 \div 4$ microns [5,6]. At the standard speeds and temperatures above 500 °C, the growth of InAs on GaAs leads to the formation of a rough surface and stacking faults. The electron mobility in the films with the thickness less than 100 nm is about 400÷1000 $cm^2/(V \cdot s)$ that is far below the mobility of the defect-free InAs.

The purpose of the present work is the development of epitaxial thin films n+InAs(Si) heavily doped with silicon and engineering of Hall effect magnetic field sensors based on this structures.

2. Material and device fabrication

2.1. Sensor material growth and properties

The structures were grown by solid-source molecular beam epitaxy Riber Compact 21T on GaAs and sapphire substrates. The samples differ by nucleation/transition layer construction (samples of the 1st, 2nd and 3rd type) located between GaAs and the doped layer of ~ 100 nm n+InAs(Si). Transition layers were introduced to optimize the epitaxial film quality before the growth of n+InAs films. For the samples on GaAs substrate GaAs buffer and superlattice AlAs/GaAs were followed by the AlGaAs layer, then, in the samples of 1st type i-InAs relaxation layers, for the 2nd type - $In_xAl_{1-x}As$ sublayer with InAs content of 75÷90 %, for the 3rd type - the metamorphic transition $In_xAl_{1-x}As$ buffer with the change of the composition from 20 to 90 % at a thickness of 1.1÷1.2 μm. 4th type sample was highly doped InAs layer grown directly on the sapphire substrate.

Since the gradual increase of InAs mole fraction up to 100% is difficult to implement due to the inertia of the cells effusion, the final part of the transition buffer is implemented as a superlattice $InAs/In_xAl_{1-x}As$. In such a structure, the sharpest drop of In composition and the maximum strain at the beginning of the InAs film growth were implemented in the structures of the 1st type. The 2nd type provided a more seamless transition from GaAs to InAs lattice. The samples of the 3rd type provided the most smooth distribution of misfit dislocations at the relaxation of $In_xAl_{1-x}As$ layer. The parameters of the samples (mobility μ and Hall electron concentration n_H) are listed in the following Table.1. The density of dislocations and stacking faults in the InAs layer affect the electron transport properties. To analyze them, the Hall concentration and the electron mobility were measured in the wide temperature range (5÷295 K).

The samples of the first type have low electron mobility and low surface roughness. The introduction of the $In_xAl_{1-x}As$ sublayer with the thickness of 25÷30 nm in the samples of the 2nd type increases the mobility of electrons by 5÷15 %. The highest electron mobility was observed in the samples of the 3rd type with the metamorphic buffer with the thickness of 1.0÷1.2 μm, as well as the largest increase in mobility at the nitrogen temperature.

The surface morphology of the films is associated with the growth conditions, temperature and pressure of arsenic. If the temperature was increased, the large defects were observed, probably due to the clusterization of the metallic In. Excess of As leads to the formation of the stacking faults and appearance of the rough surface. The optimal conditions were observed at T of about 460 °C and the pressure of arsenic of $4÷5\cdot10^{-6}$ Torr. The morphology of striated relief was not observed in the samples of the 3rd type with a thick metamorphic buffer. This is probably caused by the increase of the true temperature of the substrate due to an increase of absorption of infrared heating at the growth of layers with a high content of InAs.

Sample 346 was grown on a sapphire substrate without a transition layer. X-ray diffraction revealed the oriented polycrystalline InAs structure of this film. Due to ultra-high Si doping level and poor crystalline quality it demonstrated very low electron mobility values and negligible temperature dependence of the mobility. In turn this can be used to suppress the temperature coefficients of resistance and sensitivity.

2.2. Sensor fabrication

The sensors have a form of Greek symmetric cross performed by contact photolithography and mesa wet etching in H_3PO_4:H_2O_2:H_2O etchant. The active channel width was 200 μm. Contact metallization formed by lift-off lithography and Ti/Au (100 nm / 800 nm) vacuum deposition. The wafers have been passivated by 100 nm Si_3N_4 PECVD deposition to eliminate a surface long thermal oxidation and the damage during the followed processing. For the contact pads opening ICP dry etching of Si_3N_4 have been consequently performed. Hall sensor view is shown in Figure 1. Dies were cutted by disc saw. Au wires have been bonded by splitted electrode technique for the electrical measurements.

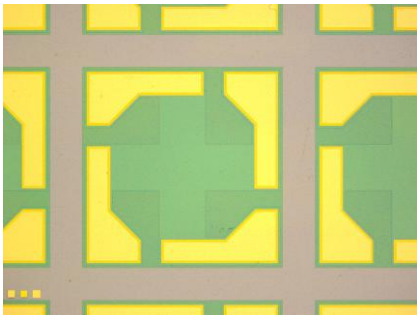

Figure 1. Hall sensor photomicrography.

3. Experimental performance

The sensors have been measured in the DC constant current regime at the different temperatures within the range 5÷295 K. Current values were 10 or 20 mA. As the Hall voltage U_H in common case is dependent on the various physical factors – temperature, magnetic field, heterostructure properties etc. Hall sensors performance is described by the series of parameters, defined as follows:

- sensitivity $S = \frac{1}{I_0}\frac{\partial U_H}{\partial B}$, where I_0 is sensor current, shown in Figure 2;
- moreover, temperature sensitivity coefficient $STC = \frac{1}{S_0}\frac{\partial S}{\partial T}$;
- resistance temperature coefficient $RTC = \frac{1}{R_0}\frac{\partial R}{\partial T}$;
- nonlinearity factor $\delta(B) = \frac{U_H(B) - U_{lin}(B)}{U_H(B)}$, where $U_{lin}(B)$ is the linear fit of experimental $U_H(B)$ dependence for the magnetic field interval 0.2-4 T. S_0 and R_0 refer to the room temperature. Low field data were excluded due to the divergence of $U_H(B)$ at $B \to 0$, accompanied by noise signals and systematic magnetic field creep embedded in the superconducting solenoid. Thus δ(B) presented the maximal nonlinearity. The dependence of δ on doping density is shown in Figure 3.

The device properties have been measured by DC current technique in CryoFree closed cycle helium cryostat with the superconductive solenoid in a magnetic field up to 6 T.

Hall sensor and material parameters measured at T=295 K are listed in Table 1.

Table 1. Material and Hall sensor properties for the different structure types measured at room temperature.

Sample	Type	n_H, 10^{13} cm^{-2}	δ, %	S, Ω/T	STC, 10^{-3} %/K	RTC, 10^{-4} %/K	μ_H, cm^2/(V·s)
162	1	1.93	0.19	32.7	3.5	23.0	5520
163	3	1.60	0.79	39.8	4.4	200	6440
252	2	3.29	0.34	19.1	2.5	19.7	3100
246	2	6.19	0.14	10.1	1.4	18.9	3620
119	1	1.05	0.03	6.0	1.8	13.1	1980
346	4	4.95	0.11	1.3	1.2	1.5	190

It can be seen from Table 1 data that the higher doping and higher electron concentration devices demonstrated lower RTC and STC. The reason is high Fermi energy due to high doping level, providing low-temperature variation of electron concentration. Resistance variation also depends on

electron mobility temperature dependence. Low electron mobility caused by high scattering rate on ionized impurities and structural defects. The highest RTC were observed in the samples with a combination of lower electron concentration and high electron mobility. In the polycrystalline sample 346 very low mobility resulted in reduced temperature variations of sensitivity and resistance.

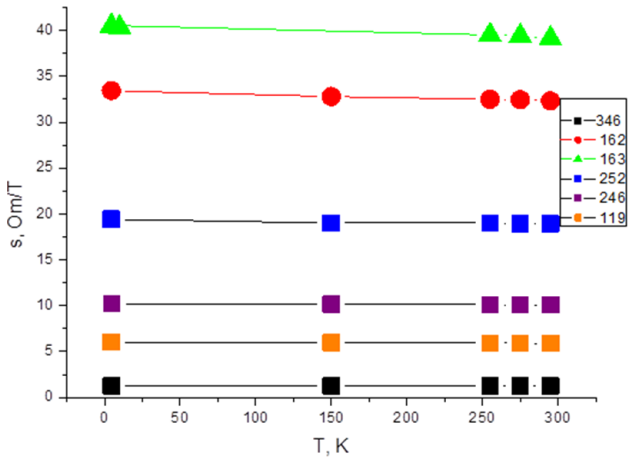

Figure 2. Temperature dependence of sensitivity for the different samples.

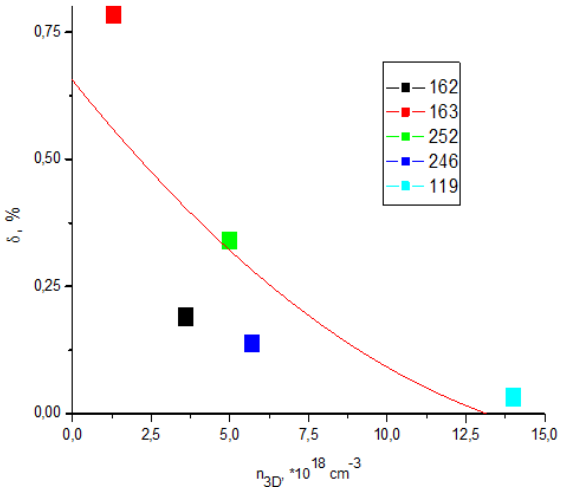

Figure 3. Correlation between nonlinearity and Si doping density.

It is worth notice that at low temperature (5÷6 K) the Hall signal and magnetoresistance hadn't demonstrated any quantum oscillations with increasing magnetic field, that usually observed in quantum well heterostructures with high electron mobility two-dimensional electron gas [7]. We account it to the relatively low mobility values due to direct InAs film doping and three-dimensional character of electron system in conductive thin films.

4. Conclusion

We have demonstrated the successful formation of highly doped InAs thin films (~100 nm) with the different intermediate layer arrangement and appropriate electron mobility values. Hall sensors have been fabricated on these structures and their performance parameters have been measured in wide temperature range. Obtained sensitivity varied from 1 to 40 Ω/T, while the best linearity and lower temperature coefficient have been found in the higher doped samples with lower electron mobility. We attribute this to the electron system degeneracy and decreased phonon contribution to electron mobility and resistance.

Acknowledgements

This work was supported by the Competitiveness Program of NRNU MEPhI.

References

[1] Bolshakova I, Vasilevskii I, Viererbl L, Duran I, Kovalyova N, Kovarik K, Kost Y, Makido O, Sentkerestiova J, Shtabalyuk A and Shurygin F 2013 *IEEE T. Magn.* **49** 50-53
[2] Bolshakova I, Belyaev S, Bulavin M, Brudnyi V, Chekanov V, Coccorese V, Duran I, Gerasimov S, Holyaka R, Kargin N, Konopleva R, Kost Y, Kuech T, Kulikov S, Makido O, Moreau P, Murari A, Quercia A, Shurygin F, Timoshyn S and Vinichenko A 2015 *Nucl. Fusion* **55**(8) 083006
[3] Okamoto A and Shibasaki I 2003 *J. Cryst. Growth* **251** 560-564
[4] Geka H, Okamoto A and Shibasaki I 2005 *J. Cryst. Growth* **278** 614-618
[5] Wang P D, Holmes S N, Le T, Stradling R A, Ferguson I T and de Oliveira A G 1992 *Semicond. Sci. Tech.* **7** 767-786
[6] Nee T E, Lin R M, Hsieh L Z and Chang L B 2002 *J. Vac. Sci. Technol. A* **20** 1128-1131
[7] Suga K, Kindo K, Ishida S, Okamoto A and Shibasaki I 2004 *Physica B* **346-347** 470-475